

Learning and composing of classical music using restricted Boltzmann machines

Mutsumi Kobayashi and Hiroshi Watanabe*

Department of Applied Physics and Physico-Informatics, Faculty of Science and Technology, Keio University, Yokohama 223-8522, Japan

Recently, software has been developed that uses machine learning to mimic the style of a particular composer, such as J. S. Bach. However, since such software often adopts machine learning models with complex structures, it is difficult to analyze how the software understands the characteristics of the composer's music. In this study, we adopted J. S. Bach's music for training of a restricted Boltzmann machine (RBM). Since the structure of RBMs is simple, it allows us to investigate the internal states after learning. We found that the learned RBM is able to compose music.

1. Introduction

Recent progress in machine learning has spurred its integration into various domains of physics. In particular, machine-learning-based methodologies are increasingly being investigated as powerful tools for data analysis, modeling, and simulation in contemporary physics research.¹⁻⁷⁾ In studies integrating physics and machine learning, there have also been attempts to understand the internal mechanisms of machine learning models from a physical perspective.³⁻⁵⁾ Among the various machine learning models, the Boltzmann machine is particularly notable for its deep relationship with physics.⁸⁾ The Boltzmann machine is an associative memory model that stores input data using spin interactions and local biases as parameters, and its operating principle is based on statistical mechanics. A restricted Boltzmann machine (RBM) is a simplified variant of the Boltzmann machine in which the network is constrained to two layers, making the learning process more tractable.^{9,10)} Applied studies of RBMs include examples such as image generation¹¹⁾ and video anomaly detection.¹²⁾ RBMs have also been employed in physics research, for instance, in studies of quantum systems.^{6,13)}

*hwatanabe@appi.keio.ac.jp

The simplicity of the RBM architecture enables us to analyze its internal mechanisms from a statistical physics perspective. This analytical accessibility, which distinguishes RBMs from more complex models, represents a key advantage in the development of explainable artificial intelligence (XAI) systems,¹⁴⁾ whose importance is increasing as AI becomes more widely deployed in society. Modern deep learning models often possess highly complex architectures, making it challenging for humans to comprehend the meaning and function of the parameters learned during training. As a result, AI systems are often operated as black boxes, with the reasoning behind their outputs remaining inaccessible to humans—a situation that has been regarded as problematic from the perspective of safety and trust.¹⁵⁾ To address this issue, research has been conducted to analyze trained models and make the basis of their outputs understandable to humans. Such analyses have also been carried out in physics research. One illustrative example of such analysis is the discovery that, when a neural network is trained to learn the temperature and spin configurations of the Ising model, its intermediate layers encode the order parameter of the system. This observation implies that the network spontaneously discovers the physical concept of an order parameter solely from the training data, without explicit supervision.⁴⁾

The applications of machine learning have progressed not only in the scientific domain but also in the field of arts, with examples such as style transfer of images by AI trained on the styles of specific painters,^{16–18)} and automatic music composition by AI.^{19–23)} In studies on machine learning-based music composition, a variety of approaches have been explored, such as generating chorales in the style of J. S. Bach²⁰⁾ and constructing large-scale language models capable of composing music,²³⁾ with trained models successfully producing original compositions. Some automatic composition systems have already reached commercial-level deployment,²²⁾ indicating that machine learning-based composition has attained a practical stage. In addition to composition, machine learning has been applied to automatic harmonization²¹⁾ and automatic accompaniment generation,²⁴⁾ expanding the possibilities for AI-assisted music production in various forms. Despite the large number of successful examples in composition, harmonization, and accompaniment, relatively few studies have analyzed the internal workings of trained music generation models,²⁵⁾ and much remains unknown about how these models internally represent and *understand* music. As interactive collaboration between humans and artificial intelligence in musical activities becomes increasingly viable, AI systems need to exhibit a level of musical understanding comparable to that of human musicians. Accordingly, elucidating how AI models perceive and process music is a matter of significant importance. A deeper understanding of the internal representations acquired dur-

ing training may not only enhance the interpretability of these models but also enable their use as analytical tools that offer novel insights into musical structure. Nevertheless, most machine learning models employed for music generation rely on complex deep learning architectures, which pose substantial challenges to the interpretability of their internal mechanisms.

In this study, we demonstrate that music composition is feasible using a restricted Boltzmann machine (RBM), a model with a simple structure that permits relatively straightforward analysis of its internal mechanisms after training. Our objective is to understand, from the perspective of statistical physics, how an RBM that performs a task not typically associated with physics, specifically music composition, internally represents musical data. Although previous work, such as that by Boulanger et al.,¹⁹⁾ has applied RBMs to music composition, few studies have explored the use of RBMs in isolation for this purpose. In the present work, we propose a method in which an RBM is trained on piano-roll representations of keyboard music. We then analyze the trained model to examine how it processes and encodes musical information, enabling it to generate compositions.

2. Method

2.1 RBM

In this study, we adopted an RBM as the model for music composition. An RBM is a Boltzmann Machine with a constrained network structure. A Boltzmann machine is a network connecting many units, each of which has spin degrees of freedom. Each edge has a weight, and each unit has a bias, which defines the energy of the network.^{8,26)} The Boltzmann machine is a type of recurrent neural network that learns patterns in input data and can then generate them stochastically. While Boltzmann machines were theoretically interesting, the learning cost increases exponentially as the number of units increases. To address the problem of the learning cost, a restricted Boltzmann machine was proposed.⁸⁾ An RBM consists of two types of layers: a visible layer and a hidden layer. It is subject to the constraint that there are no connections between units within the same layer and this constraint allows us to adopt the efficient learning procedure. Each unit has a spin degree of freedom, which can be either Gaussian-type or Bernoulli-type. A Gaussian-type unit can take continuous values ranging from minus infinity to plus infinity, whereas a Bernoulli-type unit is binary and takes only the values 0 or 1. In this study, we adopt a Bernoulli-Bernoulli RBM, in which both the visible and hidden units are of the Bernoulli type.²⁷⁾

We consider an RBM model with D visible units and P hidden units. The states of the visible and the hidden units are denoted by $\mathbf{v} = v_1, v_2, \dots, v_D$ and $\mathbf{h} = h_1, h_2, \dots, h_P$, respec-

tively, where each v_i and h_j takes a binary value of either 0 or 1. The energy of the model with the states $\{\mathbf{v}, \mathbf{h}\}$ is given by,

$$E(\mathbf{v}, \mathbf{h}|\theta) = - \sum_{i=1}^D \sum_{j=1}^P w_{ij} v_i h_j - \sum_{i=1}^D v_i b_i - \sum_{i=1}^P h_i c_i, \quad (1)$$

where, $\theta = \{w_{ij}, b_i, c_i\}$ are the model parameters.²⁸⁾ The weights $\mathbf{W} = w_{ij}$ represents the interaction between the visible unit v_i and the hidden unit h_j . The parameters $\mathbf{b} = b_i$ and $\mathbf{c} = c_i$ represent the biases of the visible and hidden layers, respectively. Given the model parameter θ , the probability of the visible layer being in the state \mathbf{v} is given by,

$$p(\mathbf{v}|\theta) = \frac{\exp\{-E(\mathbf{v}|\theta)\}}{Z(\theta)}, \quad (2)$$

where $Z(\theta)$ is the partition function defined by

$$Z(\theta) = \sum_{\mathbf{v}} \sum_{\mathbf{h}} \exp(-E(\mathbf{v}, \mathbf{h}|\theta)). \quad (3)$$

The goal of training an RBM is to make the model distribution $p(\mathbf{v}|\theta)$ approximate the data distribution $q(\mathbf{v})$ as closely as possible. To achieve this goal, we adopt the Kullback-Leibler (KL) divergence as the cost function. The KL divergence between the model distribution $p(\mathbf{v}|\theta)$ and the data distribution $q(\mathbf{v})$ is defined by

$$\text{KL}[q(\mathbf{v})|p(\mathbf{v}|\theta)] = \sum_{\mathbf{v}} q(\mathbf{v}) \log \frac{q(\mathbf{v})}{p(\mathbf{v}|\theta)}. \quad (4)$$

In general Boltzmann machines, computing the gradient of this cost function is intractable, while in the case of RBMs, it can be efficiently carried out using the Contrastive Divergence (CD) method.¹⁰⁾ In this study, we adopt the CD method as the optimization technique. We implemented the RBM model using Python, and by utilizing CuPy, we were able to accelerate the computations through GPGPU processing.²⁹⁾ The RBM code developed in this study is available on GitHub.³⁰⁾

2.2 Dataset

For the training data, we adopted compositions by J. S. Bach. A total of 58 MIDI files were obtained from the Mutopia Project,³¹⁾ and each file was converted into a black-and-white image representation known as a piano roll. A piano roll is a two-dimensional representation of musical information, where the horizontal axis corresponds to time and the vertical axis corresponds to pitch. Notes are depicted as horizontal bars, with their positions and lengths indicating the timing and duration of each note, respectively. Each pixel value in the piano roll image is either 0 or 1, corresponding to the binary visible units of a Bernoulli-type RBM.

In order to standardize the input dimensions, we restricted the training data to compo-

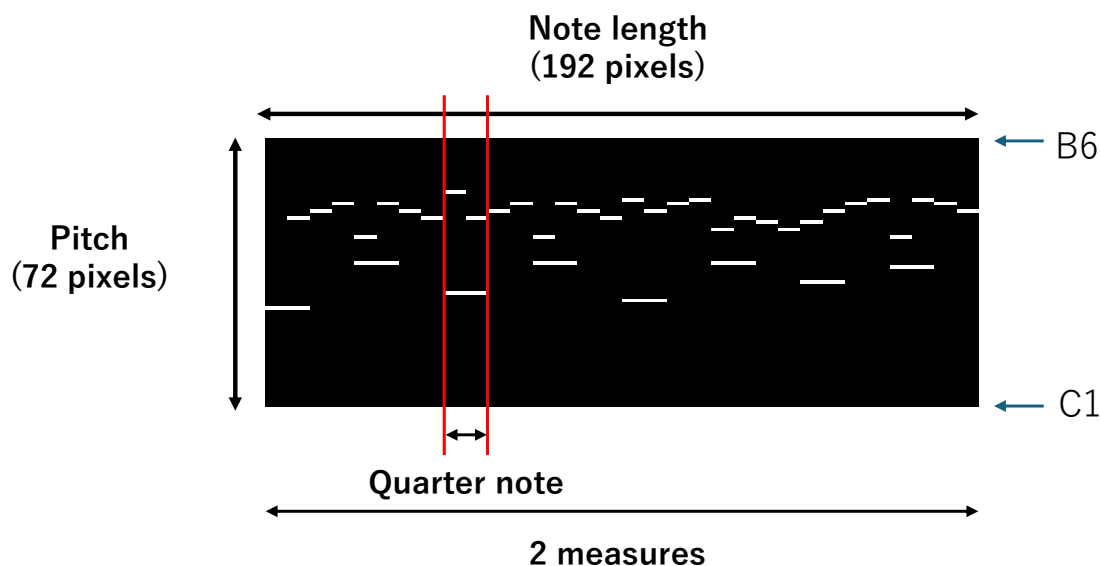


Fig. 1. (Color online) Piano roll representation of a musical segment. The horizontal axis represents time (note duration), with a total width of 192 pixels corresponding to two measures in 4/4 time. The vertical axis represents pitch, spanning 72 pixels from C1 (the lowest C on a standard 88-key piano) to B6. Each horizontal bar indicates a note, with its vertical position corresponding to pitch and its horizontal length indicating duration. A quarter note is represented by 24 pixels in width.

sitions in 4/4 time. The musical sequences were then partitioned so that each image corresponded to two measures of music.

The image size was fixed at 72×192 pixels. The vertical dimension of 72 pixels corresponds to the pitch range from C1 to B6, where C1 denotes the C note in the first octave of a standard 88-key piano (i.e., the lowest C key), and B6 denotes the B note in the sixth octave, one semitone below the highest C (C8). The horizontal dimension of 192 pixels represents time, with 24 pixels corresponding to the duration of one quarter note. This resolution was chosen so that the horizontal pixel count would be divisible by 3, enabling the representation of triplet notes.

Under this specification, the shortest representable note value is a sixty-fourth-note triplet. While this prevents accurate representation of regular sixty-fourth notes—which are the shortest notes found in the training data—their occurrence in the dataset was negligible. Moreover, this specification was adopted to keep the size of the training data computationally manageable.

During training, each piece was transposed into a total of 11 keys, including keys up to 6 semitones higher and 5 semitones lower than the original key. Through this process, a dataset

of 22,116 images for training was obtained.

2.3 Music Composition

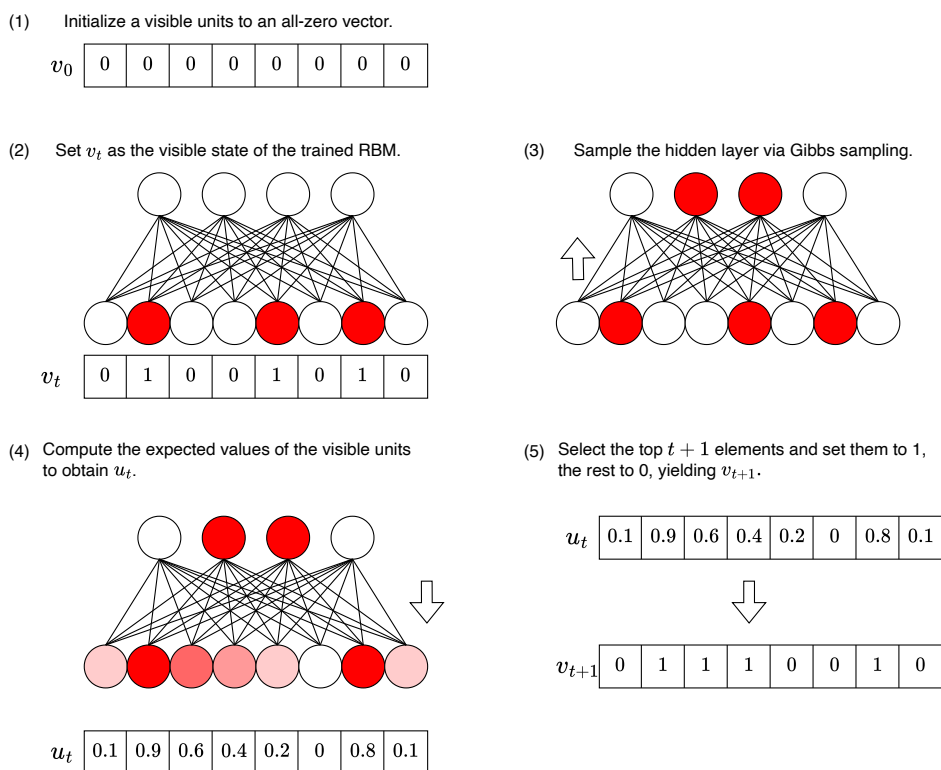


Fig. 2. (Color online) Schematic illustration of music composition procedure using the trained RBM.

We composed music using an RBM trained on piano rolls of compositions by J. S. Bach. The composition procedure is illustrated in Fig. 2 and detailed in Algorithm 1.

The number of visible units in the RBM used for training was 13,824, which corresponds to two measures in 4/4 time. Therefore, the above method allows the model to compose music up to a maximum length of two measures. To enable the RBM to generate music longer than two measures, we adopted an iterative procedure in which the latter one measure of the generated two-measure sequence are fixed and used as the first one measure for the next generation step. By repeating this procedure, the RBM is able to generate longer musical sequences. The above procedure for extending the piano roll is illustrated in Fig. 3 and detailed in Algorithm 2.

Algorithm 1 Composition Procedure

- 1: Initialize all visible units to zero and denote the resulting vector as \mathbf{v}_0 .
 - 2: Set \mathbf{v}_t as the visible state of the trained RBM.
 - 3: Given the visible units fixed at \mathbf{v}_t , the hidden unit states are sampled using Gibbs sampling.
 - 4: Compute the expected visible state \mathbf{u}_t given the sampled hidden unit states fixed.
 - 5: Construct the next visible vector \mathbf{v}_{t+1} by setting the $t + 1$ largest elements of \mathbf{u}_t to 1 and the rest to 0. Note that elements which were 1 in \mathbf{v}_t may become 0 in \mathbf{v}_{t+1} .
 - 6: By repeating steps 2 through 5 T times, a binary vector is obtained in which exactly N elements are set to 1.
-

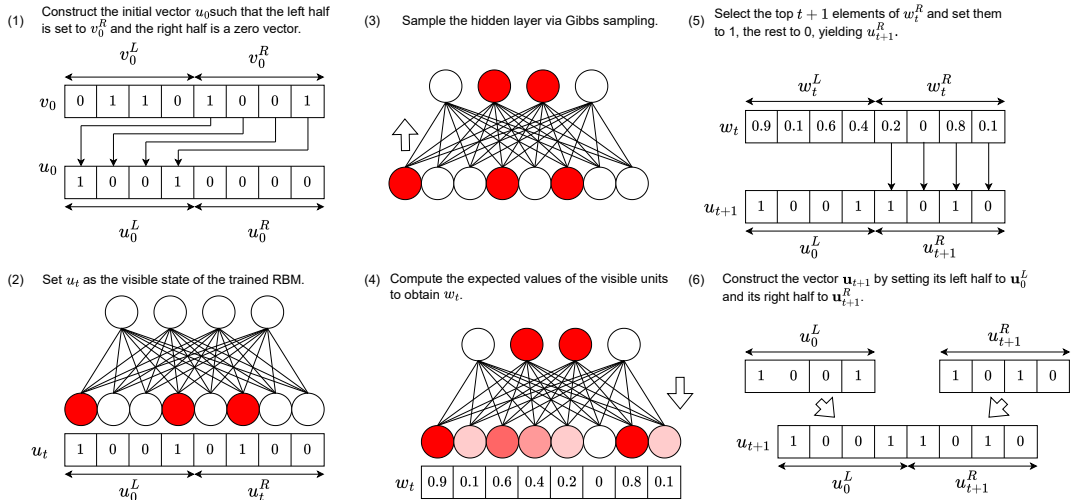


Fig. 3. (Color online) Schematic illustration of the procedure for composing a continuation from an already generated piano roll.

By using the resulting vector \mathbf{u}_N as the new initial visible vector \mathbf{v}_0 and repeating the above procedure, the piano roll can be extended further. We set $N = 1000$ for generating the initial two measures, and $N = 500$ for the process in which the right half of a measure is generated while keeping the left half fixed. This extension process was repeated six times, and the resulting images were concatenated to produce a final piano roll corresponding to eight measures of music.

Algorithm 2 Extended Composition Procedure

- 1: Generate a 72×192 pixel piano roll corresponding to four measures, and denote it by \mathbf{v}_0 .
- 2: Let $\mathbf{v}_0 = \begin{bmatrix} \mathbf{v}_0^L \\ \mathbf{v}_0^R \end{bmatrix} \in \mathbb{R}^{13824}$, where $\mathbf{v}_0^L, \mathbf{v}_0^R \in \mathbb{R}^{6912}$ correspond to the left and right halves, respectively.
- 3: Define $\mathbf{u}_0 \in \mathbb{R}^{13824}$ by:

$$\mathbf{u}_0 = \begin{bmatrix} \mathbf{u}_0^L \\ \mathbf{u}_0^R \end{bmatrix}, \quad \mathbf{u}_0^L = \mathbf{v}_0^R, \quad \mathbf{u}_0^R = \mathbf{0}.$$

- 4: Set \mathbf{u}_t as the visible state of the trained RBM.
- 5: Sample the hidden unit states using Gibbs sampling, given the visible units fixed at \mathbf{u}_t .
- 6: Compute the expected visible state \mathbf{w}_t from the sampled hidden states.
- 7: Let $\mathbf{w}_t = \begin{bmatrix} \mathbf{w}_t^L \\ \mathbf{w}_t^R \end{bmatrix}$. Select the top $t+1$ elements of \mathbf{w}_t^R , set them to 1, and the rest to 0, yielding \mathbf{u}_{t+1}^R .
- 8: Construct $\mathbf{u}_{t+1} = \begin{bmatrix} \mathbf{u}_0^L \\ \mathbf{u}_{t+1}^R \end{bmatrix}$. That is, the left half is fixed and only the right half is updated.
- 9: Repeat steps 5 through 8 for N iterations to obtain \mathbf{u}_N , in which exactly N elements in the right half are set to 1 while the left half remains unchanged.

3. Results*3.1 Reconstruction of Images Using the Trained RBM*

To verify whether the trained RBM correctly memorized the piano rolls, we input the piano roll into the visible units and examined whether it could be reconstructed through Gibbs sampling. Figure 4 shows the input piano roll images and the images obtained through reconstruction. First, when a piano roll of a J. S. Bach composition used during training was provided as input (Fig. 4 (a)), the RBM successfully reconstructed it (Fig. 4 (a')). We also provided a piano roll of a W. A. Mozart composition that was not included in the training data (Fig. 4(b)). The RBM was still able to reconstruct the image (Fig. 4(b')). From these results, we conclude that the RBM has acquired the capability to accurately reconstruct piano roll images.

To evaluate whether the RBM trained on piano rolls can reconstruct images outside the training domain, we used the MNIST dataset as input. Each 28×28 pixel image was resized to 72×192 pixels and provided to the visible units. The result of reconstruction by Gibbs sampling using the trained RBM is shown in Fig. 5. In contrast to the case of piano roll im-

ages in Fig. 4, the RBM failed to reconstruct digit images and instead produced noise-like outputs. These results indicate that the RBM trained on piano rolls is capable of reconstructing unseen piano roll images, but not images that differ in nature, such as handwritten digits. This confirms that the RBM has learned the specific features of piano roll images.

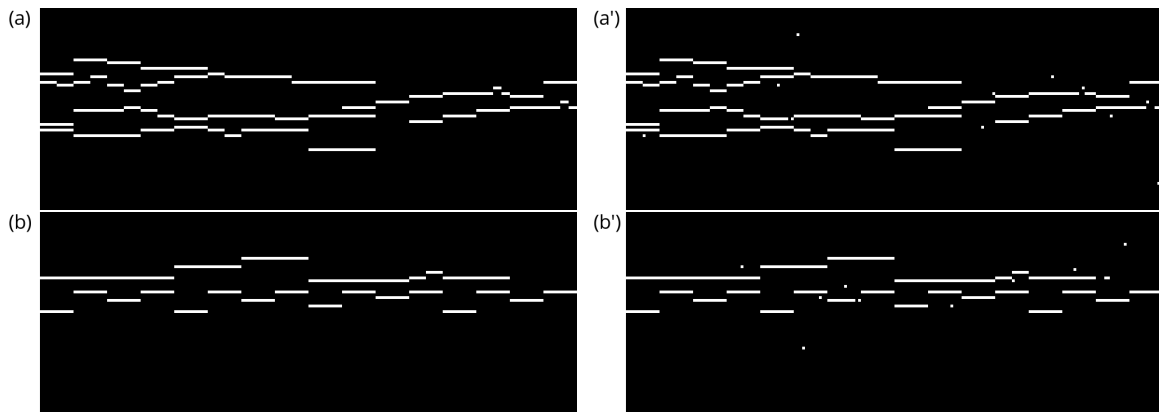


Fig. 4. Reconstruction of piano roll images by the trained RBM. (a) Piano roll image of a J. S. Bach composition used for training. (a') Image reconstructed from (a) by the trained RBM. (b) Piano roll image of a W. A. Mozart composition not used during training. (b') Image reconstructed from (b) by the trained RBM.

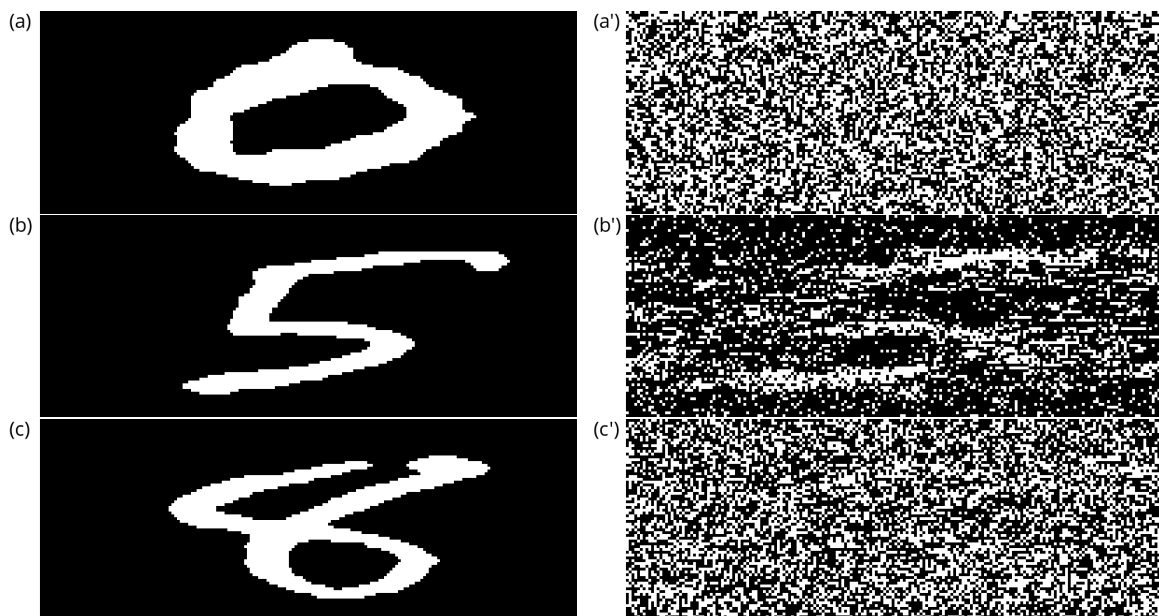


Fig. 5. Reconstruction of digit images by the trained RBM. (a), (b), (c): Input images from the MNIST dataset. (a'), (b'), (c'): Corresponding output images generated by the RBM. As evident from the outputs, the RBM fails to reconstruct the digit images and instead produces noise-like results, indicating that it has not generalized to image types outside the piano roll domain.

3.2 Energy Evaluation

To investigate how the energy of the trained RBM responds to piano roll images versus non-piano roll images, we input various types of images into the RBM and computed the corresponding energy values. Specifically, for each image, the corresponding binary vector was fed into the visible units, and the hidden units were sampled using Gibbs sampling. The energy of the RBM was then calculated from the visible and hidden states. The resulting energies for different input images are summarized in Table I. As input images, we used a piano roll included in the training data, a piano roll not used during training, three digit images from the MNIST dataset (0, 5, and 8), and white noise. We determined averages and standard deviations from 10 independent samples. As a result, piano roll images exhibited low energy values regardless of whether they were included in the training data, while other types of images generally resulted in positive energy values. Although some MNIST digit samples showed negative energy, their values were still significantly higher than those of the piano roll images. These results indicate that the RBM has learned to assign lower energy to visible unit configurations resembling piano rolls.

Table I. Energy values for different input images

Input image	Energy
Piano roll (trained)	-3654 ± 4
Piano roll (untrained)	-3353 ± 3
MNIST digit 0	44.8 ± 0.4
MNIST digit 5	-443.4 ± 1.8
MNIST digit 8	-0.1 ± 0.7
Noise	83.7 ± 0.1

3.3 Music Composition

An example of two-measure music generation using Algorithm 1 is shown in Fig. 7. The figure shows the visible states \mathbf{v}_t at sampling steps $t = 50, 100, 250, 500, 750,$ and 1000 . All images exhibit the structure of piano rolls and clearly form both chords and melodies. The time evolutions of the energy of the RBM during image generation is shown in Fig. 7. The energy decreases monotonically up to approximately 500 sampling steps, after which it begins to increase. This suggests that the RBM assigns higher energy when the number of active pixels (notes) is either too small or too large, implying the existence of an optimal number of notes that minimizes the energy.

An example of an eight-measure composition generated using Algorithm 2 is shown in Fig. 8. This image also exhibited a piano roll structure, similar to the two-measure images shown in Fig. 6. Upon listening to the music corresponding to this piano roll, we observe that although some unnatural aspects remain, the result forms a coherent piece. This indicates that even a simple RBM can successfully generate music. The audio of this piece, as well as other compositions generated by the RBM trained in this study, can be found online.³²⁾

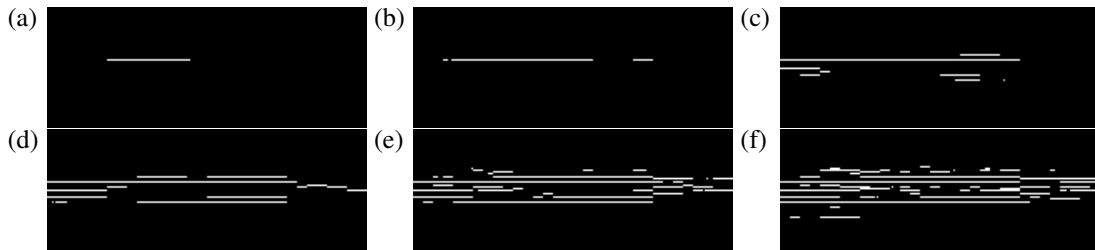


Fig. 6. Progression of the generated piano roll over sampling steps using Algorithm 1. Images (a) through (f) correspond to the visible unit states at $t = 50, 100, 250, 500, 750,$ and $1000,$ respectively.

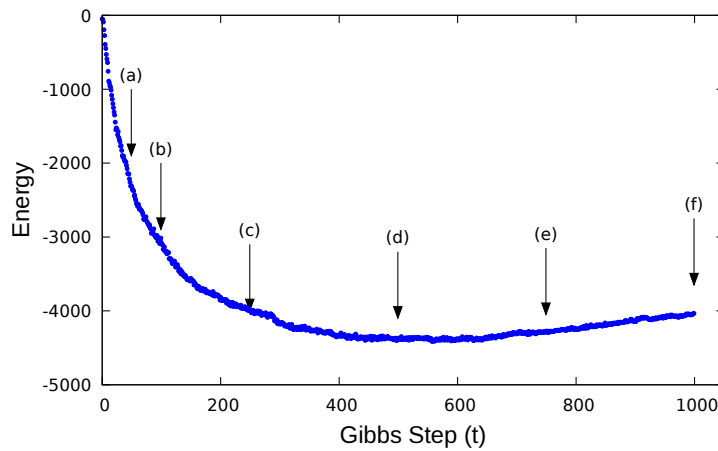


Fig. 7. Energy of each image generated at the t -th Gibbs sampling step. Labels (a)-(f) correspond to images (a)-(f) shown in Fig. 6.

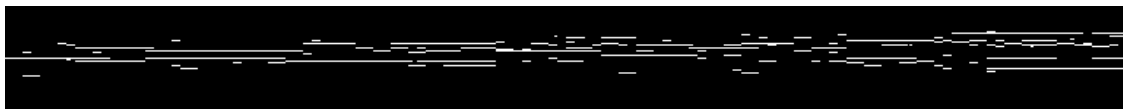


Fig. 8. Piano roll representation of an 8-measure melody composed by the RBM.

3.4 Analysis of the Hidden Layer Using *t*-SNE

We confirmed that the RBM trained on piano rolls is capable of music composition. Next, to investigate how the trained RBM internally represents musical structure, particularly whether it exhibits human-like understanding, we examined its response to transposed musical inputs. An RBM compresses the information provided to the visible layer and stores it in the hidden layer, from which the visible state can be reconstructed. This suggests that the hidden layer retains feature representations of the input. Therefore, we analyzed how the hidden layer representation changes when a musical piece is transposed.

Among the 58 compositions used for training, we selected two pieces, BWV857 and BWV868, and prepared transposed versions shifted by a semitone and a whole tone, respectively. For each version, piano roll images were generated, and multiple vectors corresponding to two-measure segments were extracted. These vectors were then provided as inputs to the visible layer of the trained RBM, and the corresponding hidden unit activations were sampled.

Figure 9 shows the result of dimensionality reduction of the hidden unit activations for each input, performed using *t*-SNE.³³⁾ When transposed by a semitone, the hidden representations corresponding to the original and transposed versions of the same piece were distributed relatively far apart (Fig. 9(a)). If the trained RBM recognized the original and semitone-transposed versions of a musical piece as the same composition, similar to human perception, then the corresponding high-dimensional hidden state vectors would be expected to be projected to nearby locations in the dimensionality-reduced space. However, the fact that the hidden states change significantly upon transposition indicates that the RBM perceives the transposed piece as an entirely different input.

To further examine the criteria by which the trained RBM evaluates musical similarity, we also analyzed the hidden states corresponding to musical data transposed up by a whole tone. The results are shown in Fig. 9(b). In contrast to the case of semitone transposition, the hidden states corresponding to the same original piece appear to be distributed in relatively close proximity. These results suggest that the trained RBM employs a notion of musical similarity that differs from that of human perception.

If the trained RBM recognizes the original music data and the music data transposed up by a semitone as the same, in a manner similar to humans, it would be expected that the pre- and post-transposition data would be plotted close to each other on the graph obtained by dimension reduction of the high-dimensional vectors in the hidden layer. However, since the pre- and post-transposition data were separated on the graph when the music was transposed

up by a semitone, it is hypothesized that the trained RBM uses a different metric than humans for recognizing the similarity between musical pieces.

To understand how the similarity between musical keys affects the internal representation of the RBM, we analyzed the number of shared scale tones between the original and transposed keys. For example, in the case of typical seven-note scales such as major and natural minor scales, transposing a piece up by a semitone results in only two common scale tones with the original key. In contrast, transposing it up by a whole tone yields five shared tones. Therefore, whole-tone transposition retains more scale tones in common with the original key than semitone transposition. This suggests a tendency for the hidden state vectors obtained from the RBM to be located closer to each other in the t-SNE projection when the transposed and original pieces share more scale tones.

These results imply that the RBM is more sensitive to the absolute pitch content rather than the relative pitch relationships of a musical input when assessing similarity. In training the RBM, we augmented the dataset by including transpositions of the original pieces up to a major sixth and down to a perfect fourth. This procedure was analogous to data augmentation in image processing, intended to encourage the model to acquire translation invariance. However, the results demonstrate that the trained RBM remains highly sensitive to pitch translations and fails to achieve invariance to transposition. The vulnerability of RBMs to translations of input data has long been pointed out,³⁴⁾ and a similar result was observed in our study using RBMs trained on piano roll data.

4. Summary and Discussion

We demonstrated that music composition is feasible even with a structurally simple model such as the RBM. By adopting the piano roll format as the data representation, we enabled the RBM to learn musical features using methods analogous to those employed for image modeling. The trained RBM was able to successfully reconstruct piano rolls, even for musical pieces that were not included in the training data. We also confirmed that the RBM fails to reconstruct images that are not piano rolls, and correspondingly assigns high energy to such inputs. Although the training data consisted of piano rolls corresponding to two measures, we developed an algorithm that allowed the model to generate musical compositions longer than two measures.

The simplicity of the RBM architecture enables us to analyze how the trained model interprets musical data more easily than with more complex models. To investigate how the RBM internally represents musical information, we analyzed the states of the hidden layer

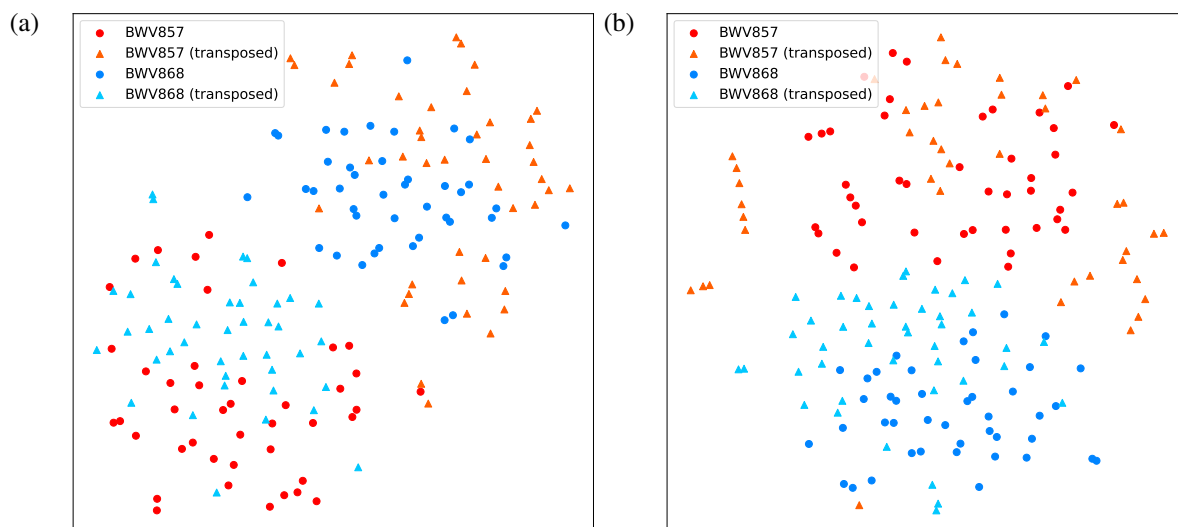


Fig. 9. (Color online) The hidden layer representations were projected into two dimensions using t-SNE. BWV 857 is shown in red and BWV 868 in blue. Original inputs are marked with circles, and transposed inputs with crosses. (a) Transposition by a semitone. (b) Transposition by a whole tone.

in response to various input data. The results suggest that transposition involves substantial changes in the hidden states, indicating that the RBM tends to assess musical similarity based more on the overlap of absolute pitch positions rather than melodic structure. It has been pointed out that RBMs and Deep Belief Networks (DBNs) lack invariance to translations in the input space. This limitation may explain the observed sensitivity to transpositions. In contrast, Convolutional Deep Belief Models, which incorporate local receptive fields and weight sharing, have the potential to recognize transposed versions of the same music as similar, due to their improved translational invariance.³⁴⁾

As a future direction, we plan to investigate whether training the RBM on compositions by composers other than J. S. Bach leads to the generation of piano roll images that exhibit different musical characteristics. This would allow us to examine whether the RBM is capable of extracting and reproducing the stylistic features specific to individual composers during the learning process. It has also been reported that the task learned by an RBM is related to the singular values of its weight matrix.³⁵⁾ Therefore, it would be an intriguing direction for future work to investigate how factors such as the composer or musical genre affect the singular value spectrum of the RBM's weight matrix.

There have been reports suggesting that each unit in the hidden layer of an RBM encodes a prototypical pattern, such as strokes in figures, in the visible layer.¹⁰⁾ However, such pat-

terns are often not clearly interpretable in standard RBMs. In contrast, Classification RBMs tend to exhibit more distinguishable and meaningful hidden-unit activations.³⁶⁾ Therefore, using Boltzmann machines with modified architectures may allow us to identify prototypical melodies or chords learned by the model. This remains an important direction for future research.

Acknowledgment

This research was supported by JSPS KAKENHI, Grant No. JP21K11923. The computation was partly carried out using the facilities of the Supercomputer Center, Institute for Solid State Physics (ISSP), University of Tokyo

Appendix: Training Time of RBM on MNIST

We developed a lightweight Python library that allows easy experimentation with RBMs. The library is available online.³⁰⁾ It performs computations using NumPy when running on a CPU and switches to CuPy to accelerate processing when a GPGPU is available. To evaluate its performance, we measured the training time of RBMs on the MNIST dataset using System C, a supercomputer at the Institute for Solid State Physics, The University of Tokyo. We measured the computation time both with and without using a GPGPU and compared the results. The CPU used was an AMD EPYC 7763 (2.45 GHz, 64 cores) with 256 GB of memory. For the GPU, we used four NVIDIA A100s, each with 40 GB of memory, totaling 160 GB of GPU memory. The results of plotting the computation time required for training RBMs with different numbers of hidden units are shown in Fig. A·1. These results indicate that using a GPGPU significantly reduces computation time.

Figure A·1 presents the computation time required to train RBMs with various numbers of hidden units. The results clearly demonstrate that GPGPU-based training significantly reduces the overall computation time compared to CPU-only execution.

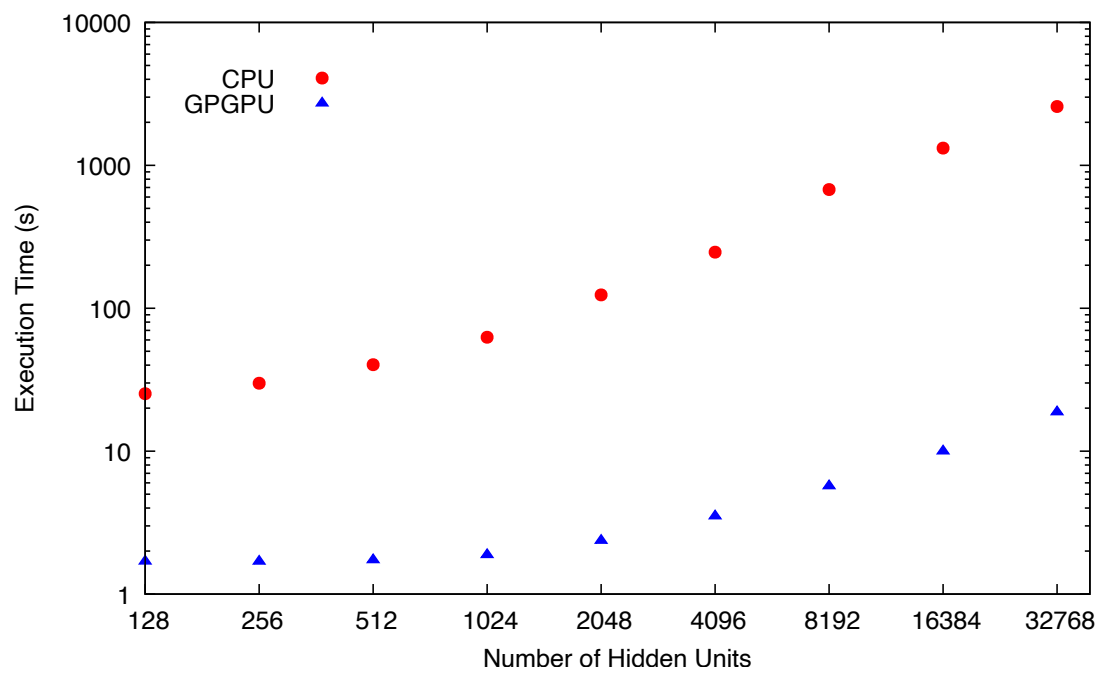


Fig. A·1. Comparison of computation time between CPU and GPGPU in training MNIST with RBM.

References

- 1) G. Torlai and R. G. Melko: Phys. Rev. B **94** (2016) 165134.
- 2) J. Carrasquilla and R. G. Melko: Nature Physics **13** (2017) 431.
- 3) H. W. Lin, M. Tegmark, and D. Rolnick: Journal of Statistical Physics **168** (2017) 1223.
- 4) K. Kashiwa, Y. Kikuchi, and A. Tomiya: Progress of Theoretical and Experimental Physics **2019** (2019) 083A04.
- 5) H. Yoshino: SciPost Phys. Core **2** (2020) 005.
- 6) Y. Nomura: Journal of Physics: Condensed Matter **33** (2021) 174003.
- 7) A. Seif, M. Hafezi, and C. Jarzynski: Nature Physics **17** (2021) 105.
- 8) D. H. Ackley, G. E. Hinton, and T. J. Sejnowski: Cognitive Science **9** (1985).
- 9) P. Smolensky et al.: *Information processing in dynamical systems: Foundations of harmony theory* (Department of Computer Science, University of Colorado, Boulder, 1986).
- 10) G. E. Hinton: Neural computation **14** (2002) 1771.
- 11) R. Liao, S. Kornblith, M. Ren, D. J. Fleet, and G. Hinton: arXiv preprint arXiv:2210.10318 (2022).
- 12) H. Vu, T. D. Nguyen, A. Travers, S. Venkatesh, and D. Phung: Pacific-Asia conference on knowledge discovery and data mining, 2017, pp. 641–653.
- 13) G. Carleo and M. Troyer: Science **355** (2017) 602.
- 14) A. Das and P. Rad: arXiv preprint arXiv:2006.11371 (2020).
- 15) W. Samek, T. Wiegand, and K.-R. Müller: arXiv preprint arXiv:1708.08296 (2017).
- 16) L. A. Gatys: arXiv preprint arXiv:1508.06576 (2015).
- 17) J. Johnson, A. Alahi, and L. Fei-Fei: Computer Vision–ECCV 2016: 14th European Conference, Amsterdam, The Netherlands, October 11–14, 2016, Proceedings, Part II 14, 2016, pp. 694–711.
- 18) D. Ulyanov, V. Lebedev, A. Vedaldi, and V. Lempitsky: arXiv preprint arXiv:1603.03417 (2016).
- 19) N. Boulanger-Lewandowski, Y. Bengio, and P. Vincent: arXiv preprint arXiv:1206.6392 (2012).
- 20) G. Hadjeres, F. Pachet, and F. Nielsen: In D. Precup and Y. W. Teh (eds), *Proceedings of the 34th International Conference on Machine Learning*, Vol. 70 of *Proceedings of Machine Learning Research*, 06–11 Aug 2017, pp. 1362–1371.

- 21) C.-Z. A. Huang, C. Hawthorne, A. Roberts, M. Dinculescu, J. Wexler, L. Hong, and J. Howcroft: arXiv preprint arXiv:1907.06637 (2019).
- 22) P. Dhariwal, H. Jun, C. Payne, J. W. Kim, A. Radford, and I. Sutskever: arXiv preprint arXiv:2005.00341 (2020).
- 23) R. Yuan, H. Lin, Y. Wang, Z. Tian, S. Wu, T. Shen, G. Zhang, Y. Wu, C. Liu, Z. Zhou, et al.: arXiv preprint arXiv:2402.16153 (2024).
- 24) Y. Ren, J. He, X. Tan, T. Qin, Z. Zhao, and T.-Y. Liu: Proceedings of the 28th ACM international conference on multimedia, 2020, pp. 1198–1206.
- 25) N. Bryan-Kinns, B. Banar, C. Ford, C. N. Reed, Y. Zhang, S. Colton, and J. Armitage: arXiv preprint arXiv:2308.05496 (2023).
- 26) G. Hinton and T. Sejnowski: Proceedings of the IEEE Conference on Computer Vision and Pattern Recognition, 1983.
- 27) T. Yamashita, M. Tanaka, E. Yoshida, Y. Yamauchi, and H. Fujiyoshii: 2014 22nd International Conference on Pattern Recognition, 2014, pp. 1520–1525.
- 28) N. Zhang, S. Ding, J. Zhang, and Y. Xue: Neurocomputing **275** (2018) 1186.
- 29) R. Nishino and S. H. C. Loomis: 31st conference on neural information processing systems **151** (2017).
- 30) M. Kobayashi and H. Watanabe. Simple RBM: A minimal implementation of Restricted Boltzmann Machine in Python. https://github.com/watanabe-appi/simple_rbm, 2025.
- 31) The Mutohia Project. The Mutohia Project. <https://www.mutopiaproject.org>, 2025. Accessed August 6, 2025.
- 32) RBM Music Demo Site. <https://watanabe-appi.github.io/rbm-music-demo/>.
- 33) L. Van der Maaten and G. Hinton: Journal of machine learning research **9** (2008).
- 34) H. Lee, R. Grosse, R. Ranganath, and A. Y. Ng: Proceedings of the 26th Annual International Conference on Machine Learning (ICML), 2009, pp. 609–616.
- 35) Y. Ichikawa and K. Hukushima: Journal of the Physical Society of Japan **91** (2022) 114001.
- 36) H. Larochelle, M. Mandel, R. Pascanu, and Y. Bengio: Journal of Machine Learning Research **13** (2012) 643.